



HAL
open science

Aluminum sampling by Chelex, titanium dioxide and zirconium oxide DGT: Influence of pH on accumulation behaviors

Juliette Rougerie, Rémy Buzier, Stéphane Simon, Gilles Guibaud

► **To cite this version:**

Juliette Rougerie, Rémy Buzier, Stéphane Simon, Gilles Guibaud. Aluminum sampling by Chelex, titanium dioxide and zirconium oxide DGT: Influence of pH on accumulation behaviors. *Environmental Technology and Innovation*, 2021, 24, pp.101931. 10.1016/j.eti.2021.101931 . hal-03859655

HAL Id: hal-03859655

<https://hal.inrae.fr/hal-03859655v1>

Submitted on 16 Oct 2023

HAL is a multi-disciplinary open access archive for the deposit and dissemination of scientific research documents, whether they are published or not. The documents may come from teaching and research institutions in France or abroad, or from public or private research centers.

L'archive ouverte pluridisciplinaire **HAL**, est destinée au dépôt et à la diffusion de documents scientifiques de niveau recherche, publiés ou non, émanant des établissements d'enseignement et de recherche français ou étrangers, des laboratoires publics ou privés.



Distributed under a Creative Commons Attribution 4.0 International License

26 **Keywords:** Aluminum speciation, Passive sampling, Binding capacity, Natural waters, Metals.

27

28 **I. INTRODUCTION**

29 The presence of aluminum (Al) in freshwaters, varying from a few $\mu\text{g L}^{-1}$ to several mg L^{-1}
30 (Habs et al., 1997), is a major concern regarding its potential toxicity. Many studies have shown that
31 it can have detrimental effects on aquatic organisms (Chassard-Bouchaud et al., 1992; Roy and
32 Campbell, 1997). If freshwaters are used as drinking water resources without removal treatment, this
33 element can also impact human health as it is considered as a risk factor for degenerative diseases
34 (Exley, 2013). The environmental effects of Al are governed by its speciation rather than its total
35 concentration. The speciation of Al mostly depends on pH (Harris et al., 1996). Acidic conditions lead
36 to the presence of cationic species such as Al^{3+} , AlOH^{2+} and $\text{Al}(\text{OH})_2^+$ which, along with weak
37 complexes (mainly inorganic), are generally recognized as the most reactive, and therefore the most
38 bioavailable forms (Gensemer and Playle, 1999). In the pH range 6.0-7.5, Al is commonly precipitated
39 as $\text{Al}(\text{OH})_{3(s)}$ (Sposito, 1995). The anionic $\text{Al}(\text{OH})_4^-$ form found in alkaline freshwaters is considered less
40 toxic than cationic species but its toxicity mechanism is not clearly known (Wilson, 2011). It should be
41 noted that the presence of ligands, such as dissolved organic matter, decreases the toxicity of Al (Roy
42 and Campbell, 1997) by limiting its bioavailability. Therefore, the toxicity of Al in freshwaters varies
43 with both pH and the presence of ligands such as organic matter (Sposito, 1995). A quantitative
44 determination of the most reactive forms of Al is thus required for a relevant toxicity risk
45 assessment.

46 The passive sampling by diffusive gradients in thin films (DGT), developed by Davison and Zhang
47 (1994), is a suitable tool for speciation studies (Menegário et al., 2017; Zhang and Davison, 2015).
48 The DGT samples only the labile fraction (*i.e.*, free element and fast-dissociating complexes) (Davison
49 and Zhang, 2012), which is considered to be the most bioavailable, thus allowing a better assessment
50 of the impacts on organisms (Røyset et al., 2005; Eismann et al., 2020). In addition, as an *in situ*

51 sampling technique, the DGT eliminates the issues associated to the sample storage by reducing the
52 risk of speciation change or contamination. Furthermore, this technique allows the determination of
53 time-weighted average concentrations and is thus more representative of organism's exposure than
54 concentrations determined from grab sampling (Allan et al., 2006), especially in dynamic systems
55 where the concentration and the speciation can vary over several hours.

56 When considering the different DGT configurations already available, various behaviors can be
57 expected for Al sampling. Several studies have shown that a conventional DGT device based on a
58 Chelex binding phase is able to sample Al, but only under acidic conditions (Panther et al., 2012;
59 Shiva et al., 2017). Another DGT, based on a titanium dioxide binding phase has also been used for Al
60 and allows its sampling under both acidic and alkaline conditions (Panther et al., 2012). It should be
61 noted that no information is yet available concerning the linear accumulation capacity of these two
62 binding phases for Al. However, this parameter is essential to ensure that there is no saturation, even
63 partial, of the binding phase which would induce an underestimation of the contamination. Such a
64 situation is particularly of concern in the case of waters with high labile Al content. It has been shown
65 that a DGT device based on a zirconium oxide binding phase has better binding capacities for several
66 oxyanions (Ding et al., 2016), but it has not been evaluated yet for Al sampling.

67 Furthermore, pH may strongly affect both the speciation of Al and the ionization state of binding
68 phase functions, consequently modifying the binding capacity. Indeed, according to pH, Al can be
69 positively charged (varying from +1 to +3), neutral or negatively charged (-1) (**Figure S1**). Concerning
70 the binding phase, depending on the pH and its pH of zero-point charge (pH_{ZPC}), it can have a
71 negative, neutral or positive global charge (**Figure S1**). These changes can lead to different binding
72 capacities: the amount of binding sites and / or the interactions between the Al species and the
73 binding phase can vary. The linear accumulation capacity of a binding phase shall thus be determined
74 considering the effect of pH.

75 In this paper, we propose an in-depth study of the accumulation capacities of DGT for Al to take
76 full advantage of its time integrative capacities in natural waters. The objectives of this work are to

77 determine the limits of linear accumulation of three binding phases (Chelex, titanium dioxide or
78 zirconium oxide) considering the effect of pH and to evaluate the DGT based on a zirconium oxide
79 binding phase as an alternative for Al sampling in freshwaters.

80 **II. MATERIALS AND METHODS**

81 **II.1. MATERIALS, REAGENTS AND SOLUTIONS**

82 All reagents were analytical grade or higher. Ultrapure water (Milli-Q system, water
83 resistivity > 18.2 MΩ.cm) was used to prepare all the solutions. All the reusable materials, including
84 the DGT devices, were cleaned by immersion in a 10% (V/V) HNO₃ bath for 24 h then rinsed with
85 ultrapure water prior to use. A 1000 mg L⁻¹ Al stock solution was prepared from Al(NO₃)₃.9H₂O
86 (Honeywell Fluka, ACS quality).

87 **II.2. DGT PROCEDURES**

88 **II.2.1. DGT SAMPLERS**

89 Three DGT binding gels were studied: Chelex-100[®] (iminodiacetic functions), Metsorb[®]
90 (titanium dioxide) and zirconium oxide. The Chelex and titanium dioxide binding gels were purchased
91 from DGT Research Ltd. The zirconium oxide binding gels were prepared according to the protocol
92 used by Devillers et al. (2017). The DGT devices were assembled using plastic holders (DGT Research
93 Ltd.) enclosing a binding gel, a polyacrylamide diffusive gel (0.78 mm thick, DGT Research Ltd.) and a
94 polycarbonate filter membrane (0.4 μm pore diameter, 0.01 mm thick, Whatman). The
95 corresponding DGT devices were labelled DGT-Ch, DGT-Ti and DGT-Zr.

96 **II.2.2. ELUTION**

97 After exposition, the DGT were dismantled and the binding gels were eluted during 24 h at
98 21 ± 1 °C in a temperature controlled room. The elution step was performed using 1 mL of 1 mol L⁻¹
99 HNO₃ for the Chelex binding gels (Warnken et al., 2007), 1 mL of 0.1 mol. L⁻¹ NaOH for the titanium

100 dioxide binding gels and 2 mL of 0.2 mol L⁻¹ NaOH for the zirconium oxide binding gels. The protocol
101 for the titanium dioxide binding gels was adapted from Bennett et al. (2010) by decreasing the NaOH
102 concentration by ten times to avoid matrix effect caused by sodium during Al analysis by atomic
103 absorption spectrometry. The protocol for the zirconium oxide binding gels was adapted from Ding
104 et al. (2016) by removing H₂O₂ to avoid apparition of zirconium oxide precipitates in the eluate over
105 time, as highlighted in their publication.

106 An elution yield of 0.84 was used for the Chelex binding gels according to Panther et al.
107 (2012) and Devillers et al. (2017). The elution yield for the titanium and zirconium oxide binding gels
108 were determined since the protocols were adapted from Bennett et al. (2010) and Ding et al. (2016),
109 respectively. For this purpose, binding gels were directly immersed in 9 mL of 10⁻² mol L⁻¹ NaNO₃
110 solution containing 50 µg L⁻¹ of Al at pH 4.0 or 8.5 (triplicates for titanium dioxide and six replicates
111 for zirconium oxide). The pH was adjusted using 1 mol L⁻¹ HNO₃ and NaOH, with addition of 5.10⁻³
112 mol L⁻¹ Na₂CO₃ for pH 8.5. After 24 h, the gels were recovered and eluted prior analysis. Samples of
113 each exposure solution were taken before and after gel immersion to determine the accumulated
114 mass of Al in each binding gel. The elution yield was calculated as the ratio between the eluted mass
115 and the accumulated mass.

116 II.2.3. DGT BLANKS

117 As Al is a ubiquitous element, the device contamination level was measured for each type of
118 DGT. For this purpose, triplicates of unexposed DGT devices were assembled, dismantled, and eluted
119 with the same procedure than applied to the exposed DGT.

120 II.3. PH INFLUENCE ON TIME-SERIES ACCUMULATION

121 To study the influence of pH only on the linear accumulation capacities, time-series
122 accumulation were performed in NaNO₃ solutions in absence of competitors. pH values close to the
123 neutrality (pH 6.0 to 7.5) could not be studied in laboratory because of the precipitation of Al,

124 impeding having a quantifiable and stable concentration. The time-series accumulation of Al by DGT
125 were consequently studied at pH 4.1, 5.3 and 8.6. These three pH allowed covering the main range of
126 dissolved inorganic Al species present in aquatic systems (**Figure S1**). To guarantee the Al
127 concentrations in the exposure solutions, they were set to the highest possible value preventing the
128 formation of insoluble $\text{Al}(\text{OH})_{3(s)}$, for each studied pH. The corresponding concentrations were 45, 17
129 and $85 \mu\text{g L}^{-1}$ for pH 4.1, 5.3 and 8.6, respectively. The ionic strength of these solutions was imposed
130 using $10^{-2} \text{ mol L}^{-1} \text{ NaNO}_3$ and the pH was adjusted using $1 \text{ mol L}^{-1} \text{ HNO}_3$ and NaOH, with addition of
131 $5 \cdot 10^{-3} \text{ mol L}^{-1} \text{ Na}_2\text{CO}_3$ for pH 8.6. Before starting the experiments, the solutions were left to
132 equilibrate for at least 72 h.

133 For each pH, DGT-Ch, DGT-Ti and DGT-Zr were deployed in a well-stirred solution at $20 \pm 1 \text{ }^\circ\text{C}$
134 using 20 L polyethylene containers (up to 24 DGT per container). The accumulation of Al was
135 evaluated over eight deployment times between 4 h and 30 days, with triplicates for each duration.
136 The pH was monitored daily and the solutions were sampled at each DGT deployment and removal
137 (or daily if no device was added/retrieved) to monitor Al concentration.

138 **II.4. DGT DEPLOYMENT IN NATURAL WATERS**

139 DGT deployments were performed in natural waters to confirm both the linear accumulation
140 capacity and the accumulation behavior of the three studied binding phases obtained in NaNO_3
141 solutions. For this purpose, three natural waters were selected for their significant dissolved Al
142 concentrations (between 100 and $300 \mu\text{g L}^{-1}$) and their pH (between 5 and 7) covering a large part of
143 the environmental range (**Table 1**). They correspond to a subsurface runoff used for drinking water
144 purpose (water C) and two rivers from headwaters located in the North-West of the Massif Central in
145 France (water M and R). More details about their physicochemical composition can be found in
146 **Table S1**.

147

148 **Table 1 : Main characteristics of the natural waters studied.** (Mean \pm SD, $n \geq 3$, DOC: Dissolved
 149 Organic Carbon)

	pH	Conductivity ($\mu\text{S cm}^{-1}$)	Dissolved Al ($\mu\text{g L}^{-1}$)	DOC (mg L^{-1})
Water C	5.0 ± 0.2	26 ± 2	290 ± 40	1.0 ± 0.7
Water M	6.0 ± 0.1	27 ± 2	97 ± 5	8 ± 1
Water R	7.1 ± 0.1	163 ± 3	260 ± 50	9 ± 4

150 Preliminary experiments showed that only DGT deployments in water C would allow to get
 151 close to the limits of linear accumulation of the studied DGT in an acceptable deployment time
 152 (*i.e.* < 2 weeks to avoid major changes in water composition). Only this natural water was therefore
 153 used to verify that the linear accumulation capacities determined in synthetic solutions are still valid
 154 in natural waters. DGT-Ch, DGT-Ti and DGT-Zr were thus deployed in triplicates in water C for two
 155 durations (4 h and 40 h) to guarantee the absence of saturation by comparing the results of short
 156 and long deployments. The longer deployment time was estimated according to **Equation 1** from the
 157 dissolved Al concentration to get close to the limit of linear accumulation obtained in the NaNO_3
 158 solution at pH 5.3.

159 In addition to the water C, the natural waters M and R were used to compare the behavior of
 160 each type of DGT in a non-saturating condition. The duration of deployment, set to stay far below the
 161 beginning of saturation of the binding gels, was chosen based on the results obtained in NaNO_3
 162 solutions and according to the DGT-available Al content of each water (estimated during preliminary
 163 experiments). DGT were thus deployed during 3 days in water M and 7 days in water R.

164 To control as much as possible the conditions during DGT deployment, the experiments were
 165 performed in the lab directly after sampling the natural waters. DGT-Ch, DGT-Ti and DGT-Zr were
 166 deployed in 5 L (for water C and M) or 20 L (for water R) of well-stirred solution in polyethylene
 167 containers. The exposition temperature was set to 6 ± 1 °C (controlled by Tinytag temperature
 168 loggers) to remain close to the field conditions (waters were sampled in winter 2021). During DGT

169 exposure, the pH and Al concentration were monitored daily. The dissolved Al concentration was
170 determined after filtration at 0.2 μm (cellulose acetate, Sartorius). In addition, ultrafiltration with a
171 low cutoff membrane (3 kDa, Vivaspin) was performed to separate large complexes from “free” Al
172 and/or small complexes. The ultrafiltration was carried out by centrifugation of 5 mL of natural
173 waters at 6000 g for 10 min at 6 ± 1 $^{\circ}\text{C}$. Filters and ultrafilters were systematically pre-conditioned
174 with 5 mL of the solution to be filtered to avoid Al sorption or release.

175 II.5. ALUMINUM MEASUREMENTS

176 II.5.1. ANALYSIS

177 The eluates and exposure solutions were analyzed by atomic absorption spectrometry with
178 electrothermic atomization (ET-AAS, Agilent 240 Z) using a platform graphite tube. A modifier
179 consisting in 0.64 mg L^{-1} (final concentration) of NH_4NO_3 and $\text{Ca}(\text{NO}_3)_2$ was used. All samples and
180 standards were acidified at 1% (V/V) with HNO_3 . The standard addition method was applied to
181 eluates of DGT exposed in natural waters to detect any potential matrix effects. For quality
182 assurance, blanks (HNO_3 1% V/V) and a control solution ($20 \mu\text{g L}^{-1}$, prepared daily) were analyzed
183 every ten samples. In addition, a $20 \mu\text{g L}^{-1}$ laboratory certified solution was analyzed at the beginning
184 and the end of each sequence (recovery > 95%). The limit of quantification of the method (according
185 to IUPAC) was estimated at $5 \mu\text{g L}^{-1}$.

186 II.5.2. C_{DGT} DETERMINATION

187 The concentration estimated by DGT, C_{DGT} ($\mu\text{g L}^{-1}$), was calculated using **Equation 1** (Davison
188 and Zhang, 1994):

$$189 C_{\text{DGT}} = \frac{m\Delta g}{DA t} \quad \text{Equation 1}$$

190 where m (ng) is the mass of Al accumulated in the binding phase, Δg is the thickness of the diffusive
191 layer (0.079 cm), t (s) is the exposure duration, A is the exposure area to solution (3.14 cm^2) and
192 D ($\text{cm}^2 \text{ s}^{-1}$) is the diffusion coefficient of Al. The values of D were taken from the literature (Panther et

193 al., 2012; Shiva et al., 2017) according to the pH of the solution and corrected according to the
194 average temperature during the deployment using the Stokes-Einstein relationship (values are listed
195 in **Table S2**).

196 II.5.3. SPECIATION CALCULATION AND STATISTICS

197 Visual MINTEQ 3.1 software was used with the default database constants to determine the
198 speciation of Al according to pH, considering $\text{Al}(\text{OH})_{3(s)}$ as the dominant solid phase ($\log K = 10.8$) and
199 equilibrium with atmospheric CO_2 . The Stockholm Humic Model (SHM) was used to simulate Al
200 interactions with organic matter in natural waters.

201 For experiments in natural waters, statistical analyses were performed to compare the results
202 obtained by each type of DGT. ANOVA tests were used to verify the equality of the means and
203 completed, if necessary, by a Student LSD (least significant difference) test to identify the different
204 means. All tests were conducted with a statistical significance level of $p = 0.05$. In addition, for
205 experiments in water C, the uncertainty of the ratios between the C_{DGT} obtained for 40 h and 4 h
206 deployment was calculated by propagation of uncertainty.

207

208 **III. RESULTS AND DISCUSSION**

209 **III.1. ELUTION**

210 **III.1.1. BLANK CONTAMINATION**

211 The eluates of unexposed DGT revealed a rather low and constant contamination
212 ($0.024 \pm 0.004 \mu\text{g}$, $0.032 \pm 0.001 \mu\text{g}$ and $0.040 \pm 0.004 \mu\text{g}$ per binding gel for DGT-Ch, DGT-Ti and
213 DGT-Zr, respectively). The mean DGT blank value was consequently systematically subtracted to the
214 results of each exposed DGT.

215 III.1.2. ELUTION YIELDS

216 There was no difference between the elution yields determined at pH 4.0 and 8.6. Values of
217 0.66 ± 0.03 ($n = 12$) and 0.65 ± 0.02 ($n = 6$) were obtained for the zirconium oxide and titanium
218 dioxide binding gels respectively. For the titanium dioxide binding gels, the elution yield obtained
219 with 0.1 mol L^{-1} NaOH was 17% lower than with 1 mol L^{-1} NaOH (Panther et al., 2012). However, this
220 adapted elution protocol allows analyzing undiluted eluates without suffering any matrix effect from
221 NaOH. In the end, it allows decreasing the quantification limit to around an accumulated mass of
222 10 ng, by avoiding the systematic ten times dilution of the original procedure.

223

224 III.2. DGT LINEAR ACCUMULATION CAPACITIES

225 III.2.1. TIME-SERIES ACCUMULATION IN NaNO_3 SOLUTIONS

226 To determine the linear accumulation capacities of each type of DGT according to pH only, the
227 accumulation of Al species by DGT-Ch, DGT-Ti and DGT-Zr was investigated in controlled NaNO_3
228 solutions at $\text{pH } 4.1 \pm 0.1$, 5.3 ± 0.1 and 8.6 ± 0.1 . Note that to avoid Al precipitation and thus control
229 the concentration of “DGT available Al”, the pH range 6.0 to 7.5 was not considered. The Al
230 speciation as a function of pH, determined using Visual MINTEQ, is given in **Table 2**. The studied
231 range of pH allowed investigating the accumulation of both cationic and anionic species.

232 The Al concentration remained stable throughout the DGT deployment, with variations lower
233 than 5%. Consequently, the DGT exposure concentration (C) used for the calculation was the mean
234 concentration of samples taken over time. The accumulated mass m (μg) was plotted as a function of
235 the deployment duration, t (day) (**Figure 1**). According to **Equation 1**, the plot of m versus t should
236 be linear, with $\text{CDA}/\Delta g$ as slope, up to the beginning of the saturation of the binding phase.
237 Therefore, for each type of DGT, the linear accumulation capacity can be determined as the m value
238 associated to the linearity disruption. Given the uncertainty between the DGT triplicates (RSD

239 generally lower than 10%), the accumulation linearity was considered lost when a difference higher
 240 than 10% was observed between the measured and the extrapolated linear value. In addition, the
 241 predicted accumulation was determined using **Equation 1** (diffusion coefficients were taken from
 242 literature according to the pH, **Table S2**) to assess the compliance of the linear accumulation with the
 243 DGT theory.

244 **Table 2: Aluminum speciation according to pH in NaNO₃ solutions, determined by Visual MINTEQ.**

pH	[Al] (µg L ⁻¹)	% of Al species				
		Al ³⁺	AlOH ²⁺	Al(OH) ₂ ⁺	Al(OH) _{3(aq)}	Al(OH) ₄ ⁻
4.1 ± 0.1	45	94.7	5.2	0.1	-	-
5.3 ± 0.1	17	44.0	38.1	16.9	0.9	0.1
8.6 ± 0.1	85	-	-	-	0.5	99.5

245
 246 At pH 4.1 (**Figure 1, a**), a linear and theoretically predictable accumulation was obtained with
 247 DGT-Ch up to 30 days. The mean accumulated mass of 15.9 µg obtained is 10% lower than the
 248 predicted one, suggesting a beginning of saturation, but staying in the limit of the accepted
 249 deviation. The limit of linear accumulation of the DGT-Ch is thus probably around 16 µg. With DGT-Ti
 250 and DGT-Zr, a linear accumulation was observed for 2 days only, up to a mass of 1.11 ± 0.07 µg and
 251 1.3 ± 0.1 µg respectively. The experimental accumulation on DGT-Ti followed the predicted trend,
 252 but a surprisingly higher accumulated mass was observed with the DGT-Zr (33% slope offset
 253 compared to prediction).

254 At pH 5.3 (**Figure 1, b**), the DGT-Ch and DGT-Ti had the same behavior, with a linear and
 255 theoretically predictable accumulation up to 20 days (accumulated mass of 4.0 ± 0.2 µg and
 256 4.6 ± 0.3 µg respectively). The mean accumulated mass for 30 days of exposition was 10% lower than
 257 the linear part, suggesting a potential beginning of saturation of both binding phases. The linear
 258 accumulation capacity of DGT-Ch and DGT-Ti can thus be estimated around 5 µg. DGT-Zr showed a
 259 slightly different behavior. Its accumulation was also linear, but the saturation did not seem to be

260 reached over the 30 days of exposition (linear accumulation up to $8.1 \pm 0.8 \mu\text{g}$). However, it should
261 be noted that the accumulation was slightly higher than the prediction (23% deviation between
262 experimental and predicted slope).

263 At pH 8.6 (**Figure 1, c**), the DGT-Ch showed a very low accumulation. These results are in
264 agreement with Panther et al. (2012) who have already observed an under-accumulation above pH
265 7.5 with this setup. The DGT-Ti and DGT-Zr presented the same behavior with a linear accumulation,
266 consistent with the theory, up to 10 days, corresponding to an accumulated mass of $11.6 \mu\text{g}$. The
267 mass of $17 \mu\text{g}$ obtained after 17 days of exposition being 15% lower than the linear part, the limit of
268 linear accumulation of DGT-Ti and DGT-Zr is thus between 11 and $17 \mu\text{g}$. At this pH, no higher
269 accumulation compared to the prediction was observed for DGT-Zr.

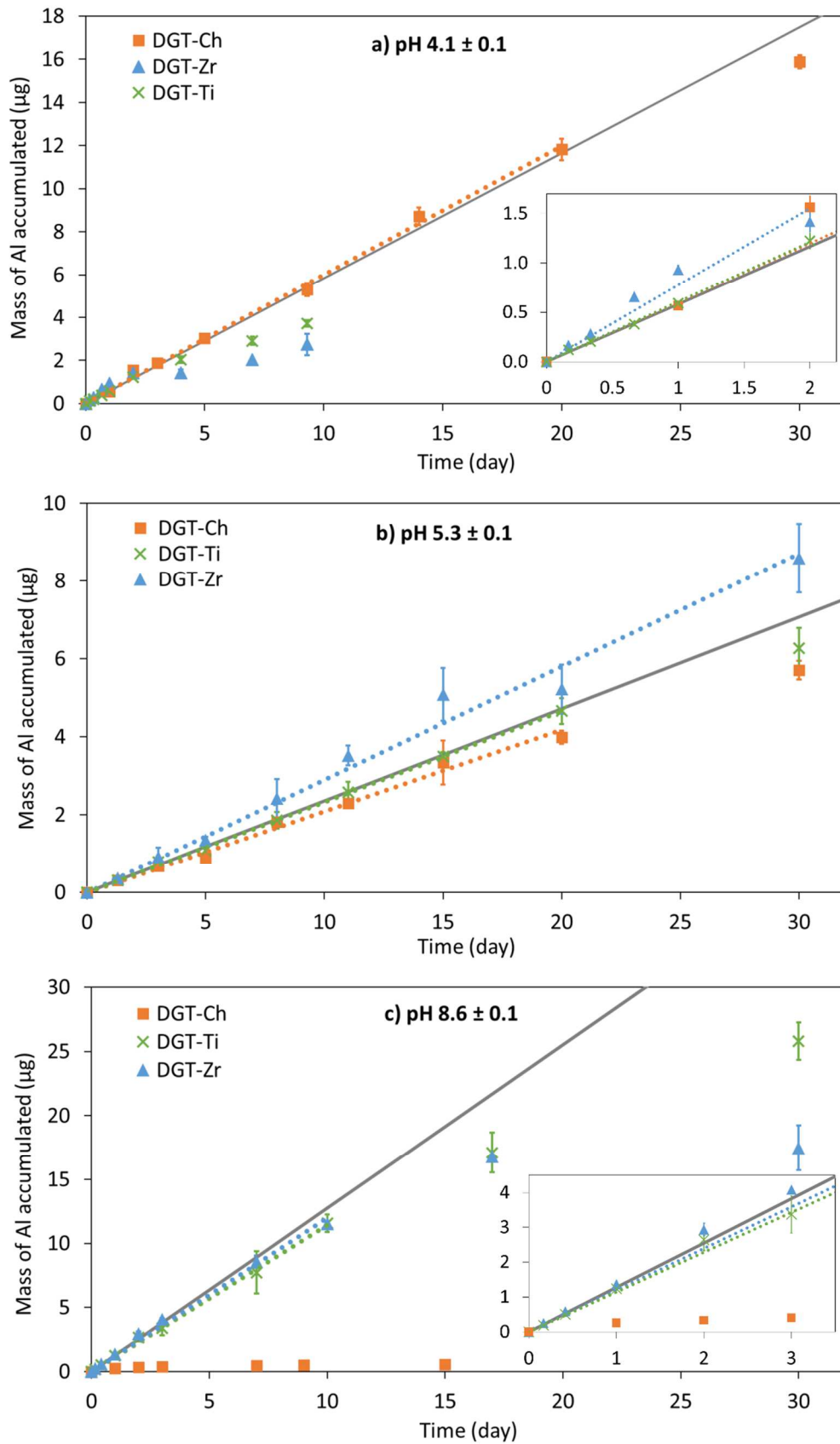


Figure 1: Accumulated mass of Al as a function of time at pH 4.1 ± 0.1 (a); 5.3 ± 0.1 (b) and 8.6 ± 0.1 (c) (mean \pm SD, $n = 3$, grey line: predicted accumulation using Equation 1, dotted lines: linear accumulation).

271 These results show that the DGT-Ch cannot be used at pH 8.6 but offers the highest linear
272 accumulation capacity at pH 4.1. The DGT-Ti and DGT-Zr can accumulate Al over the whole tested pH
273 range, with a higher linear accumulation capacity at pH 8.6. The effect of pH on both Al speciation
274 and binding phase's charge could explain the differences in accumulation capacities (**Figure S1**).
275 Indeed, Al species and the binding phase having charges of the same sign would generate
276 electrostatic repulsions, potentially resulting in a decreased accumulation capacity. In the case of the
277 Chelex binding gel, the speciation of the chelating iminodiacetic functions leads to an overall
278 negative charge above pH 6. At pH 4.1, Al is almost totally under the most positively charged species:
279 Al^{3+} (**Table 2**). It has already been demonstrated that Chelex-100 is the binding phase of choice for
280 accumulating trivalent cations (Warnken et al., 2009; Zhang and Davison, 1995). However, at pH 8.6,
281 the dissolved Al is almost totally present as the anionic form $\text{Al}(\text{OH})_4^-$ (**Table 2**) and the DGT-Ch is
282 negatively charged. Thus, Al is hardly accumulated probably due to electrostatic repulsions.

283 The charge of the titanium dioxide and zirconium oxide binding gel can be determined from
284 their pH_{ZPC} (**Figure S1**). With a pH_{ZPC} of 5.9 (Kosmulski, 2002a), the titanium dioxide is overall
285 positively charged below pH 5.9 and negatively charged above. In the literature, the pH_{ZPC} of
286 zirconium (hydr)oxide is given from 4 to 8.6, with an average and median values at 6.5 (Kosmulski,
287 2002b). Due to the different structures of the zirconium oxides, the concept of one recommended
288 pH_{ZPC} does not work particularly well (Kosmulski, 2002b). Thus, to estimate the charge of the
289 zirconium oxide phase used in our study, measurements of the zeta potential as a function of pH
290 have been performed and a pH_{ZPC} of 5.5 was determined (the procedure and values are detailed in
291 **Figure S2**). This value is in a close range of the median value proposed by Kosmulski (2002b).
292 According to our results, at pH 4.1, the DGT-Ti and DGT-Zr have a linear accumulation capacity at
293 least eight times lower than the DGT-Ch. At this pH, these two sorbents are positively charged, like
294 Al. Thus, the lowered capacity could be due to electrostatic repulsions. At pH 5.3, it clearly appears
295 that DGT-Ti and DGT-Zr have a higher linear accumulation capacity (at least 4 times higher) compared
296 to pH 4.1. At this pH, the dissolved Al species are still mostly positively charged (**Table 2**) but the two

297 sorbents are nearly neutral, therefore strongly reducing the electrostatic repulsions and thus
298 resulting in an increased accumulation capacity. However, at pH 8.6, whereas DGT-Ti, DGT-Zr and Al
299 are negatively charged, significantly higher linear accumulation capacities were determined. This
300 observation is consistent with reports of oxyanions sorption by these phases in the literature (Ding et
301 al., 2016), meaning that the potential electrostatic repulsions do not seem to significantly reduce the
302 accumulation capacity compared to pH 5.3. It should be noted that DGT-Zr was shown to accumulate
303 a higher mass of Al compared to the prediction at pH 4.1 and 5.3 but at this stage, there is no clear
304 explanation.

305 III.2.1. EXPERIMENTS IN A NATURAL WATER

306 DGT deployments were performed in the natural water C to check that the limits of linear
307 accumulation determined in NaNO₃ solutions are also valid in environmental conditions. Indeed,
308 compared to the NaNO₃ solutions used, a freshwater represents a complex matrix, with a more
309 complex speciation of Al and the presence of competitors (*e.g.* Fe, Mn, Ca, see **Table S1**) for sites
310 onto DGT binding phase. The selected freshwater has a high DGT available Al concentration that
311 allows reaching a potential saturation of the binding phases in a short duration. Two deployment
312 durations (4 h and 40 h) were compared to verify the absence of saturation.

313 For the short deployment time (4 h), the accumulated masses were lower than 1 µg, ensuring no
314 risk of saturation. After 40 h exposition, as expected, the accumulated masses (3.2 ± 0.8 , 4.5 ± 0.3
315 and 4.1 ± 0.8 µg for DGT-Ch, DGT-Ti and DGT-Zr respectively) were close to the linear accumulation
316 capacity previously determined in NaNO₃ at a similar pH (≈ 5 µg at pH 5.3). The corresponding C_{DGT}
317 value were then calculated for each deployment duration according to **Equation 1**. In case of
318 saturation, even partial, the C_{DGT} values obtained from the 40 h exposed DGT should be significantly
319 lower than the one obtained for 4 h. The ratios between C_{DGT} obtained with 40 h deployment and 4 h
320 deployment were 1.19 ± 0.24 , 1.02 ± 0.08 and 0.95 ± 0.20 for DGT-Ch, DGT-Ti and DGT-Zr,
321 respectively. These ratios are not statistically different from 1, which means that no significant

322 difference can be found between the short and long deployment duration. It can thus be concluded
323 that none of the three binding phases was saturated when accumulating $\sim 4 \mu\text{g}$ of Al. Consequently,
324 the linear accumulation capacities determined in the NaNO_3 solution appear to remain valid in this
325 type of natural water, with a more complex Al speciation and potential competitors.

326 This application in water C also highlights the importance of knowing the limit of linear
327 accumulation of DGT to properly set the deployment duration. Indeed, in this case of highly
328 contaminated water by Al, it can be nearly reached within two days of deployment, considerably
329 reducing the duration of the monitoring and the DGT time integrative capacity (which is typically
330 1 or 2 weeks).

331

332 III.3. COMPARISON OF BINDING PHASES BEHAVIORS IN NATURAL WATERS

333 To confirm the accumulation behaviors observed in NaNO_3 solutions, additional experiments
334 were performed using natural waters (waters C, M and R) with high dissolved Al concentrations, and
335 presence of organic matter (**Table 1**). To correctly compare the accumulation by each type of DGT,
336 these experiments needed to be performed in non-saturating conditions. This condition has already
337 been confirmed for experiments in the water C. For the waters M and R, the accumulated Al masses
338 were all lower than $1.2 \mu\text{g}$ (**Table S3**) and thus far below the estimated linear accumulation capacities
339 as expected. These accumulated masses were used to calculate C_{DGT} according to **Equation 1** and
340 using diffusion coefficients selected from literature (**Table S2**). The corresponding results are
341 presented in **Figure 2** with the Al concentrations determined in the natural waters after filtration
342 (“dissolved” Al) and ultrafiltration (“truly dissolved” Al).

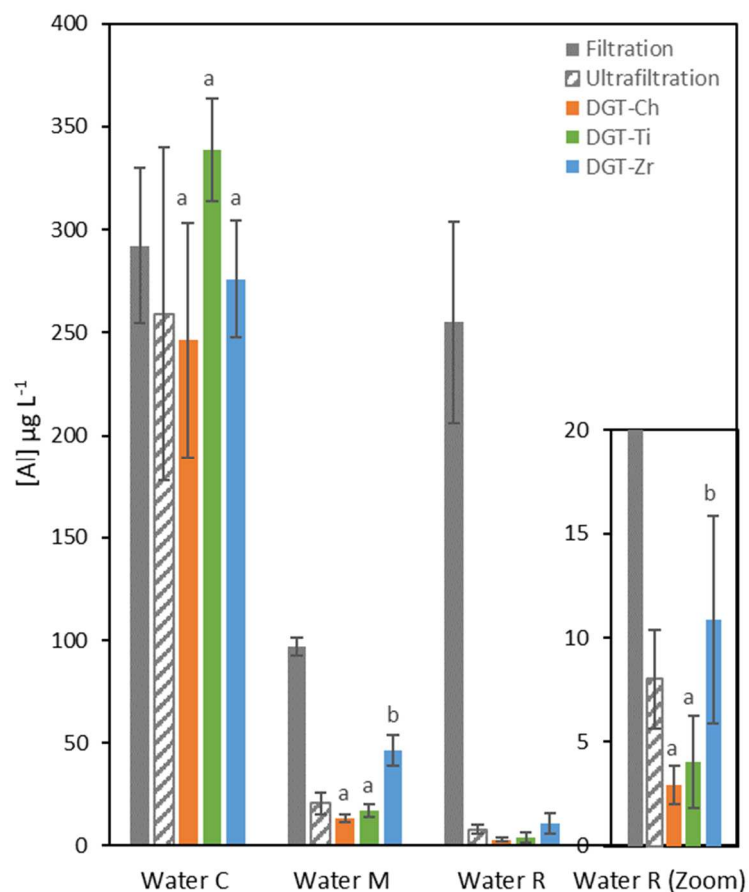


Figure 2: Concentration of Al obtained by filtration, ultrafiltration and DGT in natural waters (mean \pm SD, $n \geq 2$). For each water, the means obtained by DGT with the same letter are statistically not different.

343 In each water, the C_{DGT} obtained with DGT-Ch and DGT-Ti were in agreement, as previously
 344 observed in NaNO_3 solutions at pH 4.1 and 5.3. This seems to confirm their similar accumulation
 345 behavior of Al species between pH 4.1 and 7.1, even in the presence of organic matter. The DGT-Zr
 346 had the same accumulation behavior than DGT-Ch and DGT-Ti in the water C but led to significantly
 347 higher (about two times) accumulations in the waters M and R. After exposure in these two waters, a
 348 systematic orange coloration of the zirconium oxide binding gels was observed (**Figure S3**), indicating
 349 a potential accumulation of other compounds. The hypothesis that these compounds may induce
 350 matrix effects during the analysis was tested and discarded by performing standard addition
 351 quantifications. The significant presence of iron in waters M and R compared to water C (**Table S1**),
 352 where this phenomenon was not observed, was also suspected to induce the coloration. The

353 zirconium oxide binding gels could have accumulated iron oxyhydroxides, known to be brown-
354 orange. After elution, the gels became colorless (**Figure S3**), suggesting the potential transfer of iron
355 into the eluate. However, analysis of the eluates did not reveal any significant presence of iron. This
356 hypothesis was thus discarded. Another hypothesis could be the accumulation of other Al species by
357 the zirconium oxide binding gel (*e.g.* complexes with organic matter). For the waters M and R, the
358 ultra-filtered concentration was considerably lower than the filtered concentration (**Figure 2**),
359 indicating that most part of the dissolved Al was probably present as large-size complexes. This
360 observation can be consistent with the presence of significant organic matter in these waters (**Table**
361 **1**). In the water C with a low content of organic matter (**Table 1**), there was no significant difference
362 between the filtered and ultrafiltered concentrations (**Figure 2**), suggesting that all the aluminum
363 was “truly dissolved”. Thus, the Al complexes with organic matter are probably more present in the
364 waters M and R than in the water C. These observations are consistent with the Al speciation
365 predicted by Visual MINTEQ which shows that more than 90% of Al would be bound to organic
366 matter in waters M and R against only 25% in water C. The Al complexes with organic matter could
367 perhaps be partly accumulated by the DGT-Zr, resulting in a higher accumulation compared to DGT-
368 Ch and DGT-Ti in waters M and R.

369 **III.4. GENERAL EVALUATION OF DGT-ZR**

370 This work evaluates for the first time the DGT-Zr as an alternative for the sampling of Al. The
371 experiments revealed that the DGT-Zr could sample both cationic and anionic Al species from pH 4.1
372 to 8.6. However, in contrast to the higher capacities reported in the literature for other oxyanions
373 (Ding et al., 2016), no higher linear accumulation capacity has been observed for Al in the tested
374 conditions. In addition, compared to DGT-Ch and DGT-Ti, the use of DGT-Zr induces an over-
375 estimation of Al concentration in both NaNO₃ solutions and natural waters. Indeed, a ~30% higher
376 accumulation compared to the predicted value was observed in NaNO₃ solutions at pH 4.1 and 5.3.
377 DGT-Zr had a similarly behavior to DGT-Ch and DGT-Ti in one of the studied natural water but it

378 accumulated up to 200% more Al in the others. The potential accumulation of some organic Al
379 species by only the DGT-Zr could be assumed in the natural waters but would not explain the higher
380 accumulation observed in NaNO₃ solutions. This phenomenon observed in both synthetic and natural
381 waters for DGT-Zr cannot be explained yet. Consequently, this setup is not recommended for Al
382 monitoring without further investigations.

383 **IV. CONCLUSION**

384 By impacting both the Al speciation and the global charge of the binding phase, the pH strongly
385 affects the binding capacities of DGT. The linear accumulation capacities of DGT-Ch, DGT-Ti and DGT-
386 Zr vary up to a factor ten (from ≈1 µg to ≈15 µg) between pH 4.1 and 8.6. These capacities can easily
387 be reached within few tens of hours field deployment in freshwaters with high Al concentrations.
388 This parameter must therefore be cautiously considered to avoid DGT saturation. In contrast to what
389 could be expected, DGT-Zr did not offer higher capacity compared to DGT-Ti and, surprisingly,
390 induces an over-estimation of Al concentration in water. Consequently, the DGT-Zr is not currently
391 recommended for Al sampling.

392 Based on our results, it appears that DGT-Ti should be used for pH > 7 since DGT-Ch shows poor
393 accumulation. DGT-Ch and DGT-Ti can both be used for Al sampling at pH ≤ 7 as they present relative
394 similar accumulation behaviors in this pH range. However, the DGT-Ch should be preferred for
395 pH ≤ 5.3 and the DGT-Ti seems more suitable for pH > 5.3 because of their respective higher linear
396 accumulation capacity. The higher capacity will allow longer deployments and consequently a better
397 temporal integration of the Al contamination without the risk of DGT saturation.

398

399 **Acknowledgments**

400 The authors acknowledge Patrice Fondanèche, Karine Cleries and Emmanuelle Ducloux for
401 their contribution to the physico-chemical characterization of the natural waters.

402

403 **Funding**

404 This work was supported by the Agence de l'Eau Adour Garonne (currently, Eau Grand Sud-
405 Ouest) and the Région Nouvelle-Aquitaine.

406

407 **References**

- 408 Allan, I.J., Vrana, B., Greenwood, R., Mills, G.A., Roig, B., Gonzalez, C., 2006. A “toolbox” for biological
409 and chemical monitoring requirements for the European Union’s Water Framework
410 Directive. *Talanta* 69, 302–322. <https://doi.org/10.1016/j.talanta.2005.09.043>
- 411 Bennett, W., R Teasdale, P., Panther, J., Welsh, D., Jolley, D., 2010. New Diffusive Gradients in a Thin
412 Film Technique for Measuring Inorganic Arsenic and Selenium(IV) Using a Titanium Dioxide
413 Based Adsorbent. *Analytical chemistry* 82, 7401–7. <https://doi.org/10.1021/ac101543p>
- 414 Chassard-Bouchaud, C., Galle, Ch., Lopez-Rabereau, E., 1992. Bioaccumulation d’aluminium chez la
415 truite *Salmo trutta fario* soumise au retombées des pluies acides : étude structurale,
416 ultrastructurale et microanalytique. *Revue des sciences de l’eau* 5, 37.
417 <https://doi.org/10.7202/705119ar>
- 418 Davison, W., Zhang, H., 2012. Progress in understanding the use of diffusive gradients in thin films
419 (DGT) back to basics. *Environmental Chemistry* 9, 1–13. <https://doi.org/10.1071/EN11084>
- 420 Davison, W., Zhang, H., 1994. In situ speciation measurements of trace components in natural waters
421 using thin-film gels. *Nature* 367, 546–548. <https://doi.org/10.1038/367546a0>
- 422 Devillers, D., Buzier, R., Charriau, A., Guibaud, G., 2017. Improving elution strategies for Chelex®-DGT
423 passive samplers. *Anal Bioanal Chem* 409, 7183–7189. <https://doi.org/10.1007/s00216-017-0680-4>
- 424
- 425 Ding, S., Xu, D., Wang, Yanping, Wang, Yan, Li, Y., Gong, M., Zhang, C., 2016. Simultaneous
426 Measurements of Eight Oxyanions Using High-Capacity Diffusive Gradients in Thin Films (Zr-
427 Oxide DGT) with a High-Efficiency Elution Procedure. *Environ. Sci. Technol.* 50, 7572–7580.
428 <https://doi.org/10.1021/acs.est.6b00206>
- 429 Eismann, C.E., Menegário, A.A., Gemeiner, H., Williams, P.N., 2020. Predicting Trace Metal Exposure
430 in Aquatic Ecosystems: Evaluating DGT as a Biomonitoring Tool. *Expo Health* 12, 19–31.
431 <https://doi.org/10.1007/s12403-018-0280-3>
- 432 Exley, C., 2013. Human exposure to aluminium. *Environ. Sci.: Processes Impacts* 15, 1807–1816.
433 <https://doi.org/10.1039/C3EM00374D>
- 434 Gensemer, R.W., Playle, R.C., 1999. The Bioavailability and Toxicity of Aluminum in Aquatic
435 Environments. *Critical Reviews in Environmental Science and Technology* 29, 315–450.
436 <https://doi.org/10.1080/10643389991259245>
- 437 Habs, H., International Programme on Chemical Safety, Weltgesundheitsorganisation (Eds.), 1997.
438 Aluminium, Environmental health criteria. World Health Organization, Geneva.
- 439 Harris, W.R., Berthon, G., Day, J.P., Exley, C., Flaten, T.P., Forbes, W.F., Kiss, T., Orvig, C., Zatta, P.F.,
440 1996. Speciation of aluminum in biological systems. *Journal of Toxicology and Environmental*
441 *Health* 48, 543–568. <https://doi.org/10.1080/009841096161069>
- 442 Kosmulski, M, 2002(a). The significance of the difference in the point of zero charge between rutile
443 and anatase. *Advances in Colloid and Interface Science* 99, 255–264.
444 [https://doi.org/10.1016/S0001-8686\(02\)00080-5](https://doi.org/10.1016/S0001-8686(02)00080-5)
- 445 Kosmulski, M., 2002(b). The significance of the points of zero charge of zirconium (hydr)oxide
446 reported in the literature. *Journal of Dispersion Science and Technology* 23, 529–538.
447 <https://doi.org/10.1081/DIS-120014021>

448 Menegário, A.A., Yabuki, L.N.M., Luko, K.S., Williams, P.N., Blackburn, D.M., 2017. Use of diffusive
449 gradient in thin films for in situ measurements: A review on the progress in chemical
450 fractionation, speciation and bioavailability of metals in waters. *Analytica Chimica Acta* 983,
451 54–66. <https://doi.org/10.1016/j.aca.2017.06.041>

452 Panther, J.G., Bennett, W.W., Teasdale, P.R., Welsh, D.T., Zhao, H., 2012. DGT measurement of
453 dissolved aluminum species in waters: Comparing chelex-100 and titanium dioxide-based
454 adsorbents. *Environmental Science and Technology* 46, 2267–2275.
455 <https://doi.org/10.1021/es203674n>

456 Roy, R.L., Campbell, P.G.C., 1997. Decreased toxicity of Al to juvenile atlantic salmon (*Salmo salar*) in
457 acidic soft water containing natural organic matter: A test of the free-ion model.
458 *Environmental Toxicology and Chemistry* 16, 1962–1969. [https://doi.org/10.1897/1551-
459 5028\(1997\)016<1962:DTOATJ>2.3.CO;2](https://doi.org/10.1897/1551-5028(1997)016<1962:DTOATJ>2.3.CO;2)

460 Røyset, O., Rosseland, B.O., Kristensen, T., Kroglund, F., Garmo, Ø.A., Steinnes, E., 2005. Diffusive
461 gradients in thin films sampler predicts stress in brown trout (*Salmo trutta* L.) exposed to
462 aluminum in acid fresh waters. *Environmental Science and Technology* 39, 1167–1174.
463 <https://doi.org/10.1021/es049538l>

464 Shiva, A.H., Teasdale, P.R., Welsh, D.T., Bennett, W.W., 2017. Evaluation of the DGT technique for
465 selective measurement of aluminium and trace metal concentrations in an acid drainage-
466 impacted coastal waterway. *Environmental Science: Processes and Impacts* 19, 742–751.
467 <https://doi.org/10.1039/c6em00276e>

468 Sposito, G., 1995. *The Environmental Chemistry of Aluminum*, Second Edition. CRC Press.

469 Warnken, K.W., Davison, W., Zhang, H., Galceran, J., Puy, J., 2007. In situ measurements of metal
470 complex exchange kinetics in freshwater. *Environmental Science and Technology* 41, 3179–
471 3185. <https://doi.org/10.1021/es062474p>

472 Warnken, K.W., Lawlor, A.J., Lofts, S., Tipping, E., Davison, W., Zhang, H., 2009. In situ speciation
473 measurements of trace metals in headwater streams. *Environmental Science and Technology*
474 43, 7230–7236. <https://doi.org/10.1021/es900112w>

475 Wilson, R.W., 2011. 2 - Aluminum, in: Wood, C.M., Farrell, A.P., Brauner, C.J. (Eds.), *Fish Physiology,*
476 *Homeostasis and Toxicology of Non-Essential Metals*. Academic Press, pp. 67–123.
477 [https://doi.org/10.1016/S1546-5098\(11\)31024-2](https://doi.org/10.1016/S1546-5098(11)31024-2)

478 Zhang, H., Davison, W., 2015. Use of diffusive gradients in thin-films for studies of chemical
479 speciation and bioavailability. *Environmental Chemistry* 12, 85-
480 <https://doi.org/10.1071/en14105>

481 Zhang, H., Davison, W., 1995. Performance Characteristics of Diffusion Gradients in Thin Films for the
482 in Situ Measurement of Trace Metals in Aqueous Solution. *Analytical Chemistry* 67, 3391–
483 3400. <https://doi.org/10.1021/ac00115a005>

484

Al sampling by DGT



First evaluation for Al sampling

